Evidence for the formation of a heterotrimeric complex of leukaemia inhibitory factor with its receptor subunits in solution

Jian-Guo ZHANG*, Catherine M. OWCZAREK*§, Larry D. WARD†, Geoffrey J. HOWLETT‡, Louis J. FABRI†, Bronwyn A. ROBERTS* and Nicos A. NICOLA*‖

*The Walter and Eliza Hall Institute of Medical Research and The Cooperative Research Centre for Cellular Growth Factors, P.O. Royal Melbourne Hospital, Victoria 3050, Australia, †AMRAD Operations Pty. Ltd., Richmond, Victoria 3121, Australia, and ‡Department of Biochemistry and Molecular Biology, The University of Melbourne, Parkville, Victoria 3052, Australia

Leukaemia inhibitory factor (LIF) is a polyfunctional cytokine that is known to require at least two distinct receptor components (LIF receptor α-chain and gp130) in order to form a high-affinity, functional, receptor complex. Human LIF binds with unusually high affinity to a naturally occurring mouse soluble LIF receptor α-chain, and this property was used to purify a stable complex of human LIF and mouse LIF receptor α-chain from pregnant-mouse serum. Recombinant soluble human gp130 was expressed, with a FLAG® epitope (DYKDDDDK) at the N-terminus, in the methylotropic yeast *Pichia pastoris* and purified using affinity chromatography. The formation of a trimeric complex in solution was established by native gel electrophoresis, gel-filtration chromatography, sedimentation equilibrium analysis, surface plasmon resonance spectroscopy and chemical cross-linking. The stoichiometry of this solution complex was 1:1:1, in contrast with that of the complex of interleukin-6, the interleukin-6-specific low-affinity receptor subunit and gp130, which is 2:2:2.

INTRODUCTION

Leukaemia inhibitory factor (LIF) is a polyfunctional cytokine that acts on a wide range of cell types, including osteoblasts, hepatocytes, adipocytes, neurons, embryonal stem cells and megakaryocytes [1]. LIF exerts its biological effects by binding first to its receptor α-chain (LIFRα) with low affinity [2] and then to a second subunit molecule, gp130, to form a high-affinity, functional receptor complex [3–5]. Both LIFRα and gp130 are members of the haemopoietin or cytokine type I family of receptors [6,7]. The membrane-bound glycoprotein gp130 was initially defined as the signal transducer of the interleukin-6 (IL-6) receptor system [8,9], and has been shown subsequently to be a component of the functional receptor complexes of ciliary neurotrophic factor (CNTF) [4], oncostatin-M [3,10], cardiotrophin-1 [11,12] and interleukin-11 [13–15]. The possession of a common receptor component explains, in part, why members of this group of cytokines exert several similar and overlapping biological functions.

The signalling process through haemopoietic receptors that share gp130 is thought to involve either homodimerization of gp130 or heterodimerization of gp130 with LIFRα, leading to activation of downstream intracytoplasmic tyrosine kinases [16]. *In vitro* studies have shown that the high-affinity ternary human IL-6 receptor complex in solution consists of two molecules each of IL-6, IL-6Rα (the IL-6-specific low-affinity receptor subunit) and gp130 [17,18]. There is now evidence that CNTF also forms an IL-6-type hexameric complex with its receptor subunits, although the IL-6Rα is replaced by the CNTF receptor α-chain and the gp130 homodimer is replaced by a gp130/LIFRα heterodimer [19].

A soluble mouse LIF binding protein (mLBP) has been isolated from normal mouse serum [20,21] and found to have an N-terminal sequence identical with that of cloned mouse LIFRα (mLIFRα) [2]. Subsequent studies [22,23] have shown that the affinity of human LIF (hLIF) for recombinant mLIFRα or the naturally occurring soluble mLBP is unexpectedly high (K_D = 10–250 pM), due primarily to a very low dissociation rate (k_d = 0.0008 min^{-1}) [22]. mLIFRα or mLBP is thus able to form a highly stable binary complex with hLIF.

In order to determine the stoichiometry of the LIF receptor complex in solution, we have produced the extracellular domain of human gp130 as a recombinant soluble protein in the *Pichia pastoris* yeast expression system and purified the soluble mLIFRα in both ligated and unligated forms from mouse serum. We have demonstrated, by a variety of methods, that LIF is able to form a ternary complex with LIFRα and gp130 in solution, with a stoichiometry of 1:1:1. With all the techniques utilized, there was no evidence for the formation of a higher-order ternary complex analogous to the IL-6 system.

MATERIALS AND METHODS

Construction of a cDNA for human soluble gp130 (sgp130)

The extracellular domain of human gp130 was amplified by PCR using *Pfu* polymerase from a full-length cDNA clone (a gift from Dr. T. Taga, Tokyo Medical and Dental University, Japan). The 5′ end of the cDNA was modified to encode an *Xho*I site and an

Abbreviations used: (h)LIF, (human) leukaemia inhibitory factor; rhLIF, recombinant hLIF; (m)LIFRα, (mouse) LIF receptor α-chain; mLBP, mouse LIF binding protein; sgp130, soluble gp130; IL-6 (etc.), interleukin-6 (etc.); IL-6Rα, IL-6-specific low-affinity receptor subunit; CNTF, ciliary neurotrophic factor; FLAG® epitope, DYKDDDDK; BS^3, bis(sulphosuccinimidyl)suberate; SPR, surface plasmon resonance.

§ Present address: Molecular Genetics and Development Group, Institute of Reproduction and Development, Monash Medical Centre, Clayton, Victoria 3168, Australia.

‖ To whom correspondence should be addressed.

in-frame FLAG® epitope (DYKDDDDK). The protein began at amino acid residue 27 in the sequence of human gp130 described by Hibi et al. [9], so that the sequence at the N-terminus was DYKDDDDKPCGYIS. A stop codon was introduced immediately before the transmembrane domain at amino acid position 619, and the 3′ end was modified to encode a *Not*I site. The modified cDNA was then cloned into the yeast expression vector pPIC9 as an *Xho*I–*Not*I fragment. The pPIC9 vector contains the yeast α-factor leader sequence, which enables the heterologous protein to be secreted into the culture medium. The nucleotide sequence of the resulting plasmid pshgp130 was confirmed by dideoxy sequencing [24] using a PRISM Ready Reaction DyeDeoxy Terminator Cycle Sequencing kit on an Applied Biosystems 373 DNA sequencer.

Expression of human sgp130 in *Pichia pastoris*

The *Pichia pastoris* expression system uses the promoter from the methanol-inducible alcohol oxidase gene, *AOX1*, to express heterologous proteins. Prior to transformation into yeast, the plasmid pshgp130 was digested with *Bgl*II. This event disrupts the *AOX1* gene and results in a strain that is phenotypically Mut^s (methanol utilization sensitive). Preparation of his4 (GS115) *Pichia pastoris* sphaeroplasts and transformation of the plasmid into the host cells was carried out essentially as described [25]. Transformed colonies were selected on histidine-deficient agar plates containing 1 M sorbitol, 1 % dextrose, 1.34 % yeast nitrogen base, 0.00004 % (w/v) biotin and 0.005 % (w/v) amino acids. After incubation at 30 °C for 4–6 days, the resulting His$^+$ transformants were patched first on to a nitrocellulose filter overlaid on an agar plate (MM) containing 0.5 % methanol, 1.34 % yeast nitrogen base and 0.00004 % biotin, and then on to another agar plate (MD) containing 1 % dextrose instead of methanol as the carbon source. The plates were incubated at 30 °C. After 48 h, the clones on the MD agar plate were placed at 4 °C. The nitrocellulose filters containing the His$^+$ transformants were lifted off the MM plates and incubated in 5 % (w/v) skimmed-milk powder in 20 mM PBS (0.9 %). Colonies that expressed sgp130 were detected using a mouse anti-FLAG M2 antibody (Kodak). Clones identified in this way were grown in a shaking incubator at 30 °C to an A_{600} of 2–6 units in 10 ml of medium containing 1 % yeast extract, 2 % peptone, 100 mM potassium phosphate (pH 6.0), 1.34 % yeast nitrogen base, 0.00004 % biotin and 1 % glycerol. After 5-fold concentration by centrifugation, the cultures were resuspended in medium that contained 0.5 % methanol instead of glycerol in order to induce the yeast cells to express the heterologous protein. Expression of the recombinant protein was monitored by SDS/PAGE analysis of the supernatants of the small-scale cultures, followed by Western blotting and detection with anti-FLAG M2 antibody.

Western blotting

Proteins separated by SDS/PAGE [26] were transferred electrophoretically on to pre-wetted PVDF membranes (PVDF-Plus; Micron Separations Inc.) using a transfer buffer that contained 20 mM Tris/HCl buffer, 150 mM glycine, pH 8.2, and 20 % (v/v) methanol in a Mini-Protean II system. Blots were blocked in 5 % (w/v) skimmed-milk powder in PBS containing no sodium azide, followed by incubation with the mouse anti-FLAG M2 antibody and then with a horseradish peroxidase-conjugated rabbit anti-mouse antibody (DAKO). The bound antibody was visualized using the ECL substrate kit (Amersham) followed by autoradiography.

Purification of gp130

The cell-free supernatant (100 ml) from *Pichia pastoris* culture medium of the highest expressing clone, as determined by Western blot analysis, was applied to a 1 ml anti-FLAG M2 antibody column. After extensive washing with 10 mM Tris-buffered saline (pH 8.0) containing 0.02 % (v/v) Tween-20 and 0.02 % (w/v) sodium azide, bound sgp130 was eluted from the column with 8×0.5 ml of 50 μg/ml FLAG peptide (Kodak). The fractions containing the recombinant proteins were concentrated down to 0.5 ml using a Centricon-10 (Amicon) and subjected to gel-filtration chromatography for further purification (see below).

Purification of soluble mLIFRα (mLBP) and the binary complex between soluble mLBP and recombinant hLIF (rhLIF)

In order to generate a binary complex between mLBP and hLIF, mLBP in serum from 12-day-pregnant C57BL/6 × BL/10 mice was purified on an rhLIF affinity column. The rhLIF affinity column was generated by covalently coupling 1 mg of *Escherichia coli*-derived rhLIF (a gift from Sandoz Pharmaceutical Co., Hanover, Germany) to 1 ml of Affi-Gel 10 (Bio-Rad) according to the manufacturer's instructions. The serum was treated with Cell Debris Remover (Whatman) and then applied to the rhLIF–Affi-Gel 10 affinity column. The bound mLBP was eluted from the column by affinity elution with 0.5 mg/ml rhLIF in 20 mM Tris/HCl (pH 7.0) containing 0.02 % (v/v) Tween-20 and 0.02 % (w/v) sodium azide. Due to the high-affinity interaction between mLBP and hLIF, the affinity elution was performed by several consecutive 3–5 h incubations of the affinity column with free hLIF at 4 °C. The complex formed between mLBP and rhLIF was separated from free rhLIF and other contaminating proteins by gel-filtration chromatography (see below). Uncomplexed mLBP was obtained by the same procedure, except that elution was with ActiSep elution medium (Sterogene Bioseparations). The eluted sample was buffer-exchanged into PBS (pH 7.0) containing 0.02 % (v/v) Tween-20 and 0.02 % (w/v) sodium azide, concentrated and purified further by gel-filtration chromatography.

Gel-filtration chromatography

Protein samples of partially purified gp130, mLBP and hLIF–mLBP complex were chromatographed using a Pharmacia FPLC system on a pre-packed Pharmacia Superdex 200 gel-filtration column (300 mm × 10 mm internal diameter) operated at 0.4 ml/min in PBS containing 0.02 % (v/v) Tween-20 and 0.02 % (w/v) sodium azide. Analyses of receptor complex-formation by gel-filtration chromatography were performed on a Hewlett–Packard 1090 liquid chromatograph fitted with a model 1040A diode-array detector using a Pharmacia Superose 12 PC 3.2/30 column (300 mm × 3.2 mm internal diameter) operated at 50 μl/min at room temperature in PBS containing 0.02 % (v/v) Tween-20.

PAGE analysis

Electrophoresis on homogeneous SDS/polyacrylamide gels was performed by the method of Laemmli [26]. SDS/PAGE on 4–15 % and 8–25 % gels and native PAGE on 4–15 % gels were performed on pre-cast Pharmacia PhastGels according to the manufacturer's instructions, and the gels were visualized by silver staining [27]. Receptor complex-formation was achieved by

incubating purified human gp130, mLBP, hLIF–mLBP complex and hLIF in the desired combinations at 4 °C for at least 1 h. The complex was visualized by detection of a mobility shift in 4–15 % native PAGE by silver staining or by SDS/7.5 %-PAGE following chemical cross-linking as described below.

Analytical ultracentrifugation

Sedimentation equilibrium experiments were performed using an XLA Analytical Ultracentrifuge (Beckman Instruments, Palo Alto, CA, U.S.A.) as previously described [17]. The equilibrium profiles were measured at 230 nm for *E. coli*-derived rhLIF and mLBP and at 280 nm for the hLIF–mLBP complex. Baseline corrections were obtained by high-speed meniscus depletion experiments. The equilibrium data were analysed assuming a single solute to obtain values for the decreased molecular mass, $M(1-\upsilon\rho)$, where M is the molecular mass, υ is the partial specific volume and ρ is the solution density. The partial specific volume of rhLIF (0.747 ml/g) was calculated from the amino acid sequence. The partial specific volume of mLBP (0.702 ml/g) was calculated from the amino acid sequence [2], the sedimentation equilibrium data and using a value of 0.62 ml/g for bound carbohydrate [17]. The molecular mass and partial specific volume values obtained for mLBP imply approx. 28 % bound carbohydrate. The partial specific volume of the hLIF–mLBP complex (0.709 ml/g) was calculated assuming a 1:1 complex and no volume change on association.

Chemical cross-linking

E. coli-derived rhLIF was radio-iodinated by using a modified iodine monochloride method [28,29]. Cross-linking of ^{125}I-hLIF to mLBP or gp130 was performed by mixing the purified proteins at the indicated concentrations with radiolabelled hLIF (200000 c.p.m.) in PBS containing 50 μg/ml BSA (Pierce) in the presence or the absence of an excess of unlabelled rhLIF at 4 °C overnight. The bifunctional cross-linker bis(sulphosuccinimidyl)-suberate (BS^3) (Pierce) was added to a final concentration of 2.5 mM. The mixture was incubated at 4 °C for 30 min, and the reaction was terminated by the addition of SDS sample buffer. The cross-linked proteins were analysed by SDS/7.5 %-PAGE under non-reducing conditions, followed by autoradiography. The stable ternary complex between the purified hLIF–mLBP complex and gp130 was achieved using chemical cross-linking by incubating the hLIF–mLBP complex (70 μg/ml) with gp130 (110 μg/ml) at 4 °C for 1 h and then adding 0.5 mM BS^3 for 30 min at 4 °C. The reaction was terminated by adding Tris/HCl (pH 9.0) to 10 mM. The cross-linked proteins were resolved by SDS/PAGE on a 4–15 % gel under non-reducing conditions, and the gel was visualized by silver staining.

Detection of interactions of immobilized gp130 with hLIF and the hLIF–mLBP complex by surface plasmon resonance (SPR) spectroscopy

The interactions of hLIF and the hLIF–mLBP complex with gp130 were monitored by SPR using a BIAcore 2000® instrument. sgp130 was immobilized on the sensor chip as previously described [17], and samples were passed sequentially over the sensor surface derivatized with gp130 or with ethanolamine (blank). Signals observed on the blank chip were subtracted from those on the gp130 chip to derive specific response units. Kinetic analysis was performed by non-linear regression analysis using the BIAEvaluation program 2.1 (Pharmacia Biosensor AB). Due to the rapid rate of dissociation of the complexes, no regeneration of the sensor chip surface was required between exposure cycles. All assays were performed at a flow rate of 5 μl/min in 10 mM Hepes (pH 7.4) containing 0.15 M NaCl, 3.4 mM EDTA and 0.005 % (v/v) Tween-20.

Protein estimation

Protein concentrations were determined by amino acid analysis on a Beckman 6300 high-performance amino acid analyser equipped with a model 7000 data analyser (Beckman).

RESULTS AND DISCUSSION

Production of human sgp130 FLAG fusion protein in *Pichia pastoris*

In order to produce and purify sufficient human sgp130 for use in the study of the ternary hLIF–mLBP–gp130 complex, a cDNA for human gp130 was modifed to encode a FLAG® epitope at the N-terminus and a stop codon immediately before the predicted transmembrane domain. The truncated protein therefore lacked the cytoplasmic and transmembrane domains, but retained the immunoglobulin-like domain, the haemopoietin domain and all three fibronectin type III domains of the native receptor [2,6,7]. The modified cDNA was then subcloned into the yeast expression vector pPIC9 and transformed into his4 (GS115) *Pichia pastoris* sphaeroplasts.

Recombinant human sgp130 was purified from the cell-free culture supernatant of a high-expressing His^+ transformant using an anti-FLAG M2 antibody column and gel-filtration chromatography (Figure 1). It was estimated that 170 μg of purified gp130 was obtained from 100 ml of culture medium. SDS/PAGE analysis of the purified protein from the gel-filtration column revealed several protein bands between 85 and 115 kDa (Figure 1, inset), suggesting that the sgp130 produced in *Pichia pastoris* was variably glycosylated.

Binary-complex-formation between hLIF and mLBP

The formation of a complex between hLIF and mLBP was investigated by native PAGE, gel-filtration chromatography, chemical cross-linking and analytical ultracentrifugation. Soluble

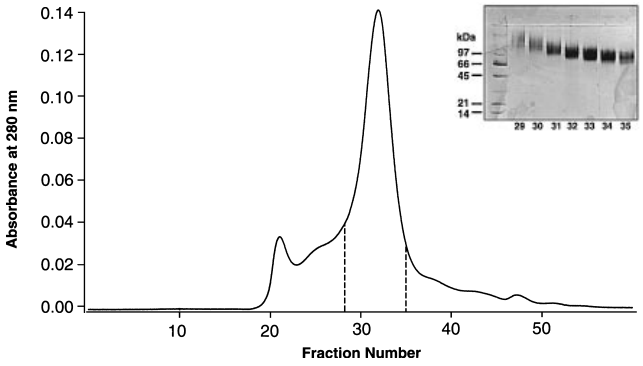

Figure 1 Gel-filtration profile of the purification of gp130 using an anti-FLAG M2 column

Eluates of gp130 from the M2 affinity column were concentrated using a Centricon-10 and applied on to a Superdex 200 column. The sample was eluted at a flow rate of 0.4 ml/min, and 0.4 ml fractions were collected. Inset: SDS/PAGE analysis of fractions 29–35 (between the vertical broken lines). The samples were prepared by mixing equal volumes of each fraction with 2 × SDS sample buffer, with loading of 1 μl/lane. Electrophoresis on an 8–25% polyacrylamide gel in the presence of SDS was performed as described in the Materials and methods section. The most concentrated fractions (fractions 32–34) were pooled and used in the study.

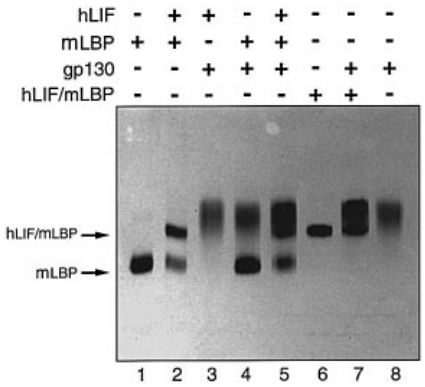

Figure 2 Receptor complex-formation monitored by native gel electrophoresis

The protein concentrations of each component alone or in the reaction mixtures were as follows: lane 1, mLBP (90 μg/ml); lane 2, mLBP (90 μg/ml) + hLIF (125 μg/ml); lane 3, gp130 (70 μg/ml) + hLIF (125 μg/ml); lane 4, mLBP (90 μg/ml) + gp130 (70 μg/ml); lane 5, mLBP (90 μg/ml) + gp130 (70 μg/ml) + hLIF (125 μg/ml); lane 6, hLIF–mLBP complex (hLIF/mLBP; 85 μg/ml); lane 7, hLIF–mLBP complex (85 μg/ml) + gp130 (70 μg/ml); lane 8, gp130 (70 μg/ml). The loading was 1 μl/lane. Electrophoresis on a 4–15% native gel was performed as described in the Materials and methods section.

mLBP purified from mouse serum migrated as a single band (Figure 2, lane 1) on 4–15% native PAGE. Upon incubation with hLIF (5-fold molar excess), an additional band (Figure 2, lane 2) was observed. This new band was not the added hLIF itself, as hLIF (pI > 9.0) did not migrate into the gel under the experimental conditions used. In addition, this band migrated to the same position as the hLIF–mLBP complex (Figure 2, lane 6) isolated from a hLIF affinity column by competitive affinity elution with hLIF, indicating that mLBP had formed a stable complex with hLIF. Not all of the mLBP participated in complex formation even in the presence of a 5-fold molar excess of hLIF, suggesting that some of the receptor (approx. 25–50%) was inactivated during the purification process. This is consistent with our previous observation that mLBP is susceptible to denaturation under various elution conditions [20]. It is worth noting that no detectable free mLBP was observed in the purified hLIF–mLBP complex, confirming our previous finding that mLBP forms a highly stable complex with hLIF in solution [22].

We attempted to determine the stoichiometry of the hLIF–mLBP complex using gel-filtration chromatography. As shown in Figure 3, hLIF (Figure 3A), mLBP (Figure 3B) and the hLIF–mLBP complex (Figure 3D) each eluted as single peaks. After mixing mLBP with a 5-fold molar excess of hLIF, the elution position of mLBP (Figure 3E) did not change significantly compared with that of mLBP alone (Figure 3B). However, SDS/PAGE analysis of fractions across this peak indicated that hLIF co-eluted with mLBP (results not shown), suggesting that hLIF–mLBP complex-formation had occurred. A comparison of the elution position of a mixture of mLBP and hLIF (Figure 3E) with that of the purified hLIF–mLBP complex (Figure 3D) revealed a small, but reproducible, difference in elution time. A combination of the elution times of the complexed mLBP and the remaining free mLBP (probably representing the inactivated portion of mLBP) was likely to be the cause of this difference.

Calculation of molecular masses based on the migration of marker proteins of known molecular mass yielded estimates of 12.9, 190 and 218 kDa for hLIF, mLBP and the hLIF–mLBP complex respectively. We knew that hLIF interacted weakly with the gel-filtration column used; as a result, the observed apparent

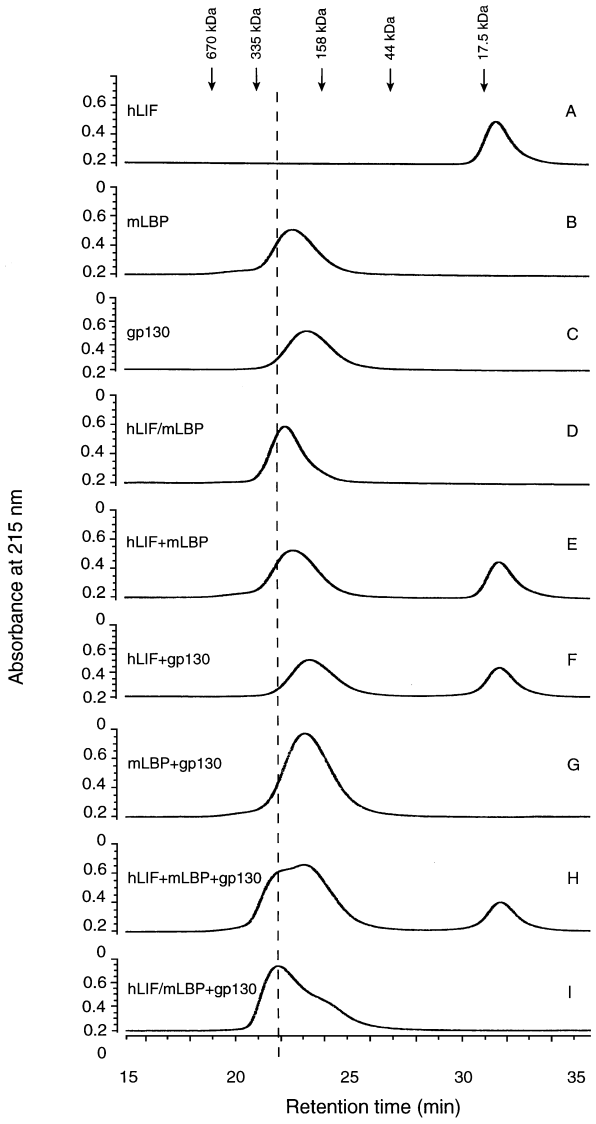

Figure 3 Gel-filtration chromatographic analyses of receptor complexes of LIF

The chromatographic conditions are given in the Materials and methods section. Samples with one or more than one component were prepared by incubating the protein(s) in the desired combinations in a final volume of 25–32 μl at 4 °C for at least 30 min before being applied on to the column. (**A**) hLIF (3 μg); (**B**) mLBP (3 μg); (**C**) gp130 (3 μg); (**D**) hLIF–mLBP complex (hLIF/mLBP; 3 μg); (**E**) hLIF (3 μg) + mLBP (3 μg); (**F**) hLIF (3 μg) + gp130 (3 μg); (**G**) mLBP (3 μg) + gp130 (3 μg); (**H**) hLIF (3 μg) + mLBP (3 μg) + gp130 (3 μg); (**I**) hLIF–mLBP complex (3 μg) + gp130 (3 μg). The elution position of the ternary complex is indicated by the vertical broken line. The arrows indicate the elution positions of the molecular mass markers (equine myoglobin, 17.5 kDa; chicken ovalbumin, 44 kDa; bovine γ-globulin, 158 kDa; thyroglobulin monomer, 335 kDa; thyroglobulin dimer, 670 kDa).

molecular mass of hLIF is smaller than the calculated value of 19960 Da. The molecular mass values for mLBP and the hLIF–mLBP complex were, however, much higher than expected. By SDS/PAGE, the apparent molecular mass of mLBP was 102.2 kDa (see Figure 7), and therefore the expected molecular mass of the hLIF–mLBP complex should be about 122 kDa. Initially we thought that mLBP might exist as a non-covalently linked dimer under native conditions (gel filtration; Figure 3) and may dissociate into monomers under denaturing conditions (SDS/PAGE; see Figure 7). If so, the stoichiometry of the

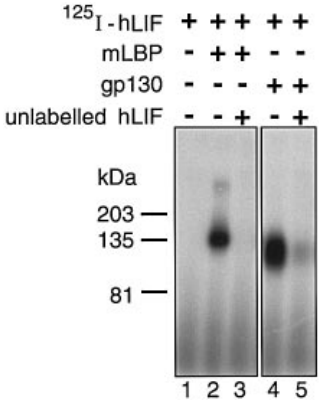

Figure 4 Chemical cross-linking of ^{125}I-hLIF to mLBP and gp130

Purified mLBP (0.6 μg/ml) or gp130 (0.5 μg/ml) was cross-linked to ^{125}I-hLIF (200000 c.p.m.) in the absence or the presence of excess unlabelled hLIF, as described in the Materials and methods section. The samples were analysed by SDS/7.5%-PAGE under non-reducing conditions, followed by autoradiography. The migration of the molecular mass markers (in kDa) is indicated on the left.

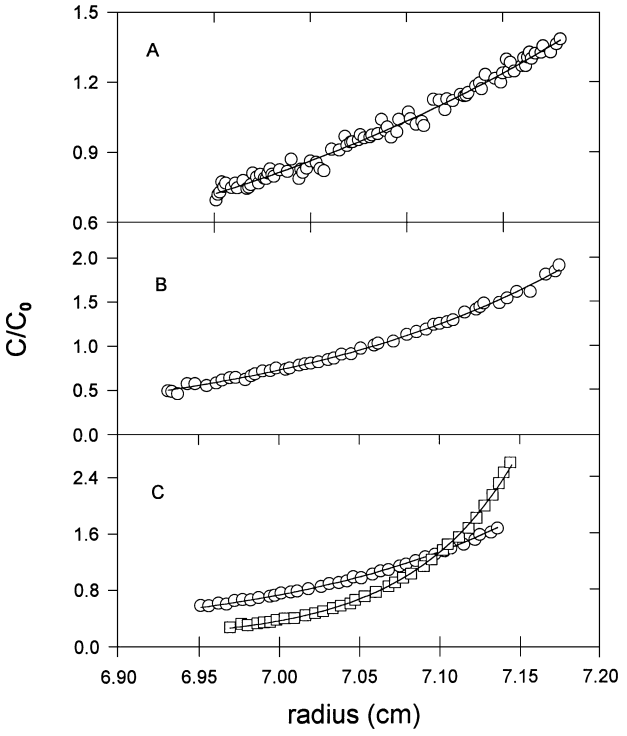

Figure 5 Determination of the molecular masses of hLIF, mLBP and the hLIF–mLBP complex by sedimentation equilibrium analysis

All analyses were performed at 20 °C in PBS containing 0.02% (v/v) Tween-20. The initial concentrations of hLIF, mLBP and the hLIF–mLBP complex were 50, 50 and 30 μg/ml respectively. (**A**) hLIF, 15000 rev./min; (**B**) mLBP, 8000 rev./min; (**C**) hLIF–mLBP complex, 8000 rev./min (○) and 12000 rev./min (□). The solid lines, computed for single solutes, yield values of 20.7, 106 and 116.1 kDa for the molecular masses of hLIF, mLBP and the hLIF–mLBP complex respectively. C and C_0 are the concentration at the given radius and the initial concentration of the solutes respectively.

hLIF–mLBP complex would be either one or two hLIF molecules bound to one mLBP dimer. This would explain the higher molecular masses of mLBP (190 kDa) and the hLIF–mLBP complex (218 kDa) obtained on gel filtration under native conditions.

To test these possibilities, and to obtain more accurate molecular mass estimates for mLBP and the hLIF–mLBP complex, we performed chemical cross-linking and analytical ultracentrifugation studies. Figure 4 shows that cross-linking of ^{125}I-hLIF to mLBP yielded a major band with an apparent molecular mass of $\sim$135 kDa (lane 2). This value, in reasonable agreement with the expected molecular mass of 122 kDa for the complex, suggested that mLBP was largely a monomer. Sedimentation equilibrium analysis (Figure 5) strongly supported this conclusion. The molecular mass obtained for hLIF (20.7 kDa) is in close agreement with the value obtained from the amino acid sequence (19.96 kDa). The sedimentation equilibrium distributions for mLBP and the hLIF–mLBP complex yielded molecular mass values of 106 and 116.1 kDa respectively. The molecular mass of the complex is close to that predicted for a 1:1 complex (122 kDa), and is consistent with previous findings [22,23]. Since apparent molecular masses from gel-filtration chromatography are highly dependent on molecular shape (hydrodynamic volume) [30], the discrepancy between the values obtained by sedimentation equilibrium and gel filtration suggest that mLBP and the hLIF–mLBP complex may have rather elongated shapes.

Specific interaction between hLIF and gp130

It has been shown previously that hLIF interacted directly with a chimaeric protein composed of the extracellular domain of human gp130 and the human IgG_1 constant region [31,32]. When we analysed the possible interaction between hLIF and gp130 using native PAGE and gel-filtration chromatography, such an interaction was not observed. As shown in Figure 2, no significant difference in either the electrophoretic mobility or the staining intensity of the band could be detected for gp130 alone (lane 8) compared with gp130 mixed with hLIF (lane 3). Also, chromatography of gp130 together with hLIF (Figure 3F) did not show an altered elution position of the gp130 peak (Figure 3C). SDS/PAGE analysis of fractions across the gp130 peak (Figure 3F) indicated that there was no detectable hLIF co-eluting with gp130 (results not shown). However, when chemical cross-linking was performed, we were able to show an interaction between gp130 and ^{125}I-hLIF (Figure 4, lane 4). The interaction was specific, as the cross-linking of ^{125}I-hLIF to gp130 was inhibited by an excess of unlabelled hLIF (Figure 4, lane 5). The apparent molecular mass of the cross-linked band was calculated to be 120 kDa, suggesting a 1:1 complex between ^{125}I-hLIF (apparent molecular mass $\sim$20 kDa) and gp130 (the average apparent molecular mass of gp130 was about 91 kDa as estimated by SDS/PAGE; see Figures 1 and 7).

The ability of gp130 to interact with hLIF was investigated further in real time using a biosensor. sgp130 was immobilized to the carboxylated dextran matrix coating the gold sensor chip, and the binding of hLIF was monitored upon its introduction to the sensor surface. Non-specific binding to the sensor surface was estimated based on the SPR signal measured on passage over a non-derivatized sensor surface, and this signal was subtracted electronically from the signal on the test surface. The sensorgrams presented in Figure 6(A) correspond to the specific interaction of hLIF (0.14–10 μg/ml) with immobilized gp130. Equilibrium binding analysis of the data (Figure 6C) yielded a K_D of 44 nM, suggesting that the binding of hLIF to gp130 was of low affinity. A similar value of 31.1 ± 0.5 nM was calculated from the ratio of the association and dissociation rate constants, with values of $(7.7 \pm 0.1) \times 10^5$ $M^{-1} \cdot s^{-1}$ and $(2.4 \pm 0.01) \times 10^{-2}$ s^{-1} being cal-

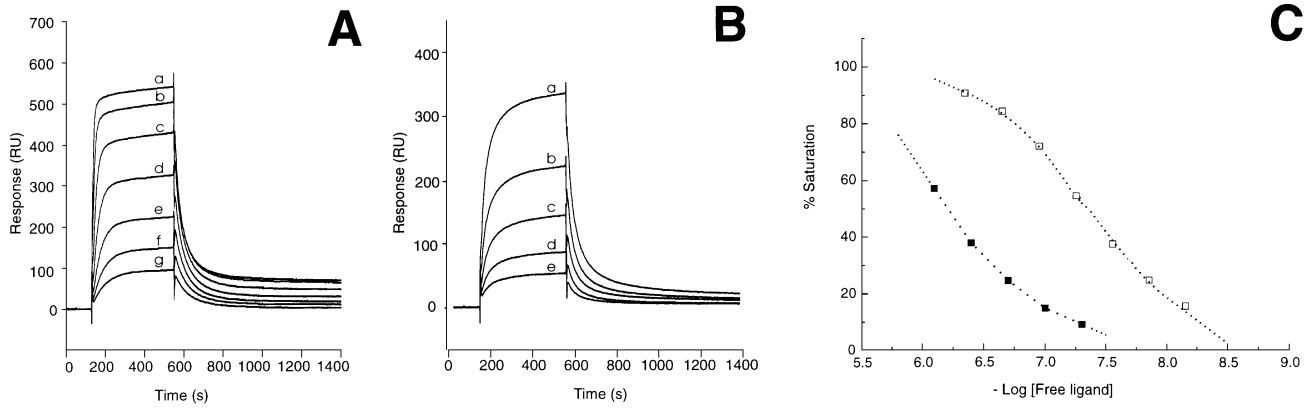

Figure 6 Characterization of the binding of hLIF and the hLIF–mLBP complex to immobilized gp130 using a biosensor employing SPR

(**A**) Sensorgrams a–g correspond to hLIF concentrations of 10, 5.0, 2.5, 1.25, 0.64, 0.32 and 0.14 μg/ml respectively. (**B**) Sensorgrams a–e correspond to hLIF–mLBP concentrations of 88, 44, 22, 11 and 5 μg/ml respectively. (**C**) Dependence of percentage saturation of hLIF (■) and hLIF–mLBP (□) on the free ligand concentration. Lines of best fit, calculated using non-linear regression analysis, correspond to a theoretical relationship assuming $K_D = 44$ nM for hLIF and $K_D = 598$ nM for the hLIF–mLBP complex. RU, response units.

culated for k_a and k_d respectively. The relatively high dissociation rate could explain why we did not observe any interaction between hLIF and gp130 by native PAGE and gel filtration, the rate constant being high in relation to the time taken for separation.

Stoichiometry of the hLIF–mLBP–gp130 complex

We first investigated the ability of sgp130 to participate in the formation of a ternary complex with LIF and soluble mLIFRα (mLBP) by native PAGE (Figure 2). When gp130 (Figure 2, lane 8) was mixed with an equivalent amount of purified hLIF–mLBP binary complex, a significant decrease was observed in the staining intensity of the hLIF–mLBP complex band, with a corresponding increase in the intensity of a broad band that migrated at a similar position to that of gp130 alone (Figure 2, compare lanes 6–8). When gp130 was incubated with either hLIF (Figure 2, lane 3) or mLBP (Figure 2, lane 4) alone, there was no significant change in the electrophoretic mobility or differential decrease in the intensity of these bands. When uncomplexed mLBP, gp130 and hLIF were mixed together, the intensity of the free mLBP band decreased and an enhanced staining intensity corresponding to the complex was again observed (Figure 2, lane 5), thus indicating that the interaction between gp130 and the hLIF–mLBP complex was specific.

We then analysed the interaction of gp130 with the purified hLIF–mLBP complex or of hLIF with a mixture of mLBP and gp130 using gel-filtration chromatography. As shown in Figure 3, the elution positions of gp130 and hLIF–mLBP were incompletely separated from each other, but could be reproducibly distinguished. Similarly, equimolar mixtures of these two species generated a bimodal elution profile, with the two apparent peaks incompletely resolved from each other; however, the higher-molecular-mass peak had a reproducibly earlier elution time (represented by the vertical broken line in Figure 3) than either hLIF–mLBP or gp130 (compare Figures 3C, 3D and 3I). When hLIF, mLBP and gp130 were chromatographed together, this higher-molecular-mass peak again appeared (Figure 3H). The slight, but reproducible, shift in elution position of the high-molecular-mass species relative to that of hLIF–mLBP suggested the formation of a 1:1 complex between hLIF–mLBP and gp130. Any other combinations of hLIF, mLBP and gp130 did not produce this peak. Re-chromatography of this new peak following collection of the appropriate fractions resulted in the main peak shifting to the elution position of the hLIF–mLBP complex, with a minor shoulder corresponding to gp130 (results not shown). This suggests that the high-molecular-mass complex formed was unstable and dissociated during re-chromatography. Because of this, we were unable to isolate this complex in a pure form for determination of its stoichiometry by ultracentrifugation. However, preliminary results from sedimentation equilibrium analysis of an equimolar mixture of hLIF–mLBP and gp130 agreed with the conclusion of a 1:1:1 complex between hLIF and its receptor subunits (results not shown).

The formation of a ternary complex between hLIF–mLBP and gp130 in solution was analysed further by the chemical cross-linking approach. We incubated purified hLIF–mLBP complex with a molar excess of gp130 to form a complex, which was stabilized by addition of the cross-linker BS^3. The cross-linked proteins were then analysed by SDS/PAGE. Figure 7 shows that cross-linking of gp130 to the hLIF–mLBP complex produced a new band with an apparent molecular mass of 200 kDa (lane 2). Treatment of gp130 or the hLIF–mLBP complex alone with the cross-linker did not generate any similar bands (Figure 7, lanes 4 and 6). The molecular mass of 200 kDa for the complex agreed very well with the sum of the molecular mass estimates for gp130 ($\sim$ 91 kDa on average; Figure 7, lane 4) and hLIF–mLBP complex ($\sim$ 109 kDa on average; Figure 7, lane 6). These data were consistent with gp130 forming a 1:1 ternary complex with the hLIF–mLBP complex in solution.

Although hLIF binds to mLIFRα with high affinity [22,23,33], it cannot transduce a biological signal in the absence of gp130 [33]. However, a functional receptor complex can be generated when either human or mouse gp130 is present, even without a further significant increase in binding affinity [33]. To estimate the binding affinity between the hLIF–mLBP complex and human sgp130, we used a biosensor approach as described above. An overlay of the sensorgrams for the specific interaction of the hLIF–mLBP complex (5–88 μg/ml) with immobilized gp130 is presented in Figure 6(B). Non-specific binding to the sensor surface was determined using a blank chip, as described above for hLIF binding. Equilibrium binding analysis of the data

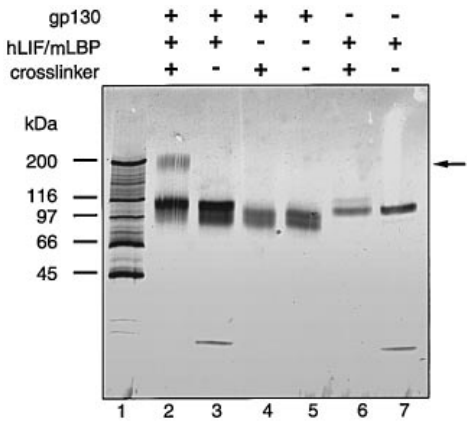

Figure 7 Ternary-complex-formation of hLIF–mLBP–gp130 as assessed by chemical cross-linking

Details of the cross-linking are given in the Materials and methods section. The cross-linked samples were analysed by SDS/PAGE on a 4–15% gel, which was visualized by silver staining. The migration positions of the molecular mass markers (in kDa) are shown on the left. The arrow indicates the position of the ternary complex.

(Figure 6C) gave a K_D of 598 nM, suggesting that the binding of hLIF–mLBP to gp130 is of very low affinity. Similarly, a K_D value of 486 ± 33 nM was calculated from the ratio of the respective rate constants, with k_a and k_d values of $(5.4 \pm 0.3) \times 10^4$ $M^{-1} \cdot s^{-1}$ and $(2.6 \pm 0.02) \times 10^{-2}$ s^{-1} being determined. Binding was specific and dependent on LIF ligation, since uncomplexed mLBP did not interact with immobilized gp130 or inhibit the binding of the hLIF–mLBP complex to gp130 on the sensor chip (results not shown). These results, similar to those reported previously for the IL-4 receptor system [34], where IL-4 first binds to the IL-4 receptor α-chain with high affinity (K_D = 100–850 pM [35–37]) and then the common γ-chain (γ_c) binds to this complex with low affinity ($K_D = \sim 1$–10 μM) to form the heterotrimeric complex, are consistent with a stepwise mechanism for the interaction of these receptor molecules.

However, the measured affinity (K_D = 598 nM) for the interaction of hLIF–mLBP with gp130 appeared inconsistent with the fact that a specific interaction of hLIF–mLBP with gp130 was detected by native PAGE and gel-filtration chromatography, while the interaction between gp130 and hLIF (with an equilibrium dissociation constant of 44 nM) was not detected using the same methods. It is unlikely that this inconsistency was caused by the attachment of the 900 Da, highly charged FLAG epitope to the N-terminus of the gp130 molecule, because similar results were obtained in subsequent studies using a non-FLAG-tagged gp130 produced in CHO cells (J.-G. Zhang and N. A. Nicola, unpublished work). The most likely explanation is that the interaction between gp130 and the hLIF–mLBP complex, but not hLIF, was detected by native PAGE and gel-filtration chromatography because the hLIF–mLBP complex and gp130 were only partially resolved from the hLIF–mLBP–gp130 ternary complex, thus facilitating their continuing interactions during the separation processes, whereas hLIF and gp130 were separated completely by these methods.

In summary, the experiments described in the present study provide the first direct evidence for tripartite complex formation between LIF, LIFRα and gp130 in solution. The stoichiometry of the complex was 1:1:1. There was no evidence suggesting complex formation of LIF with its receptor subunits with a stoichiometry of 2:2:2. In contrast, the related cytokine receptor complex for IL-6 has been shown to have a stoichiometry of 2:2:2 in solution (IL-6–soluble IL-6Rα–gp130) [17,18], and the CNTF receptor complex has a stoichiometry of 2:2:1:1 (CNTF–CNTF receptor α-chain–gp130–LIFRα) [19]. On the other hand, the soluble IL-4 receptor complex has a stoichiometry of 1:1:1 (IL-4–IL-4 receptor α-chain–γ_c) [34], and even the dimeric IL-5 cytokine forms a soluble receptor complex with a stoichiometry of 1:1 with soluble IL-5 receptor α-chain [38,39], while the growth hormone–growth-hormone receptor complex has a stoichiometry of 1:2 [40].

However, it should be borne in mind that the complex that we have studied contains LIF and gp130 from human but LBP from mouse, so we cannot eliminate the possibility that the stoichiometry of the complex may be limited by species-specific interactions. Indeed, one of the reasons for using this complex was the very high affinity of hLIF for mLBP compared with human LIFRα [22,23], which allows a stable complex to be formed. Evidence from several laboratories suggests that hLIF may have two sites of interaction with human LIFRα [22,41] and that these contacts are more stable in the hLIF complex with mLIFRα [22]. It is possible that these additional contacts could mask other interactions that might occur in the all-human complex.

Nevertheless, hLIF is fully active on mouse cells bearing LIF receptors, so it is clear that even the cross-species interactions are fully functional, presumably as a 1:1:1 complex. Consequently, it appears that a signalling-competent receptor complex consists of either a gp130 homodimer or a LIFRα/gp130 heterodimer. In the former case, IL-6/IL-6Rα dimers drive gp130 dimerization, whereas in the latter case a single LIF molecule causes LIFRα/gp130 heterodimerization. In the LIF-related cytokine family, the formation of gp130 homodimers or gp130 heterodimers seem to be mutually exclusive, and these two events give rise to similar but distinguishable signalling events [42].

We thank Sandoz for *E. coli*-derived rhLIF, T. Taga for providing the gp130 cDNA clone, J. Eddes and R. J. Simpson for amino acid analysis, and S. Olding for preparing the Figures. This work was supported by the Australian Federal Government Cooperative Research Centres Program; the National Health and Medical Research Council, Canberra, Australia; and the National Institutes of Health, Bethesda, MD (grant CA-22556).

REFERENCES

1 Nicola, N. A. and Hilton, D. J. (1997) in Growth Factors and Cytokines in Health and Disease, Vol. 2B (LeRoith, D. and Bondy, C., eds.), pp. 605–660. JAI Press, Greenwich, CT
2 Gearing, D., Thut, C. J., VandenBos, T., Gimpel, S. D., Delaney, P. B., King, J., Price, V., Cosman, D. and Beckmann, M. P. (1991) EMBO J. **10**, 2839–2848
3 Gearing, D. P., Comeau, M. R., Friend, D. J., Gimpel, S. D., Thut, C. J., McGourty, J., Brasher, K. K., King, J. A., Gillis, S., Mosley, B., Ziegler, S. F. and Cosman, D. (1992) Science **255**, 1434–1437
4 Ip, N. Y., Nye, S. H., Boulton, T. G., Davis, S., Taga, T., Li, Y., Birren, S. J., Yasukawa, K., Kishimoto, T., Anderson, D. J., Stahl, N. and Yancopoulos, G. D. (1992) Cell **69**, 1121–1132
5 Davis, S., Aldrich, T. H., Stahl, N., Pan, L., Taga, T., Kishimoto, T., Ip, N. Y. and Yancopoulos, G. D. (1993) Science **260**, 1805–1808
6 Bazan, J. F. (1990) Proc. Natl. Acad. Sci. U.S.A. 87, 6934–6938
7 Cosman, D. (1993) Cytokine **5**, 95–106
8 Taga, T., Hibi, M., Hirata, Y., Yamasaki, K., Masuda, T., Hirano, T. and Kishimoto, T. (1989) Cell **58**, 573–581
9 Hibi, M., Murakami, M., Saito, M., Hirano, T., Taga, T. and Kishimoto, T. (1990) Cell **63**, 1149–1157
10 Gearing, D. P. and Bruce, A. G. (1992) New Biol. **4**, 61–65
11 Pennica, D., King, K., Shaw, K. J., Luis, E., Rullamas, J., Luoh, S.-M, Darbonne, W. C., Knutzon, D. S., Yen, R., Chien, K. R., Baker, J. B. and Wood, W. (1995) Proc. Natl. Acad. Sci. U.S.A. **92**, 1142–1146
12 Pennica, D., Shaw, K. J., Swanson, T. A., Moore, M. W., Shelton, D. L., Zioncheck, K. A., Rosenthal, A., Taga, T., Paoni, N. F. and Wood, W. (1995) J. Biol. Chem. **270**, 10915–10922

13 Yin, T., Taga, T., Tsang, M. L., Yasukawa, K., Kishimoto, T. and Yang, Y. C. (1993) J. Immunol. **151**, 2555–2561
14 Fourcin, M., Chevalier, S., Lebrun, J.-J., Kelly, P., Pouplard, A., Wijdenes, J. and Gascan, H. (1994) Eur. J. Immunol. **24**, 277–280
15 Hilton, D. J., Hilton, A. A., Raicevic, A., Rakar, S., Harrison-Smith, M., Gough, N. M., Begley, C. G., Metcalf, D., Nicola, N. A. and Wilson, T. A. (1994) EMBO J. **13**, 4765–4775
16 Kishimoto, T., Taga, T. and Akira, S. (1994) Cell **76**, 253–262
17 Ward, L. D., Howlett, G. J., Discolo, G., Yasukawa, K., Hammacher, A., Moritz, R. L. and Simpson, R. J. (1994) J. Biol. Chem. **269**, 23286–23289
18 Paonessa, G., Graziani, R., De Serio, A., Savino, R., Giapponi, L., Lahm, A., Salvati, A. L., Toniatti, C. and Ciliberto, G. (1995) EMBO J. **14**, 1942–1951
19 De Serio, A., Graziani, R., Laufer, R., Ciliberto, G. and Paonessa, G. (1995) J. Mol. Biol. **254**, 795–800
20 Layton, M. J., Cross, B. A., Metcalf, D., Ward, L. D., Simpson, R. J. and Nicola, N. A. (1992) Proc. Natl. Acad. Sci. U.S.A. **89**, 8616–8620
21 Yamaguchi-Yamamoto, Y., Tomida, M. and Hozumi, M. (1993) Leukemia Res. **17**, 515–522
22 Layton, M. J., Lock, P., Metcalf, D. and Nicola, N. A. (1994) J. Biol. Chem. **269**, 17048–17055
23 Tomida, M. (1995) J. Biochem. (Tokyo) **117**, 1228–1231
24 Sanger, F., Nicklen, S. and Coulson, A. R. (1977) Proc. Natl. Acad. Sci. U.S.A. **74**, 5463–5467
25 Cregg, J. M., Barringer, K. J., Hessler, A. Y. and Madden, K. R. (1985) Mol. Cell. Biol. **5**, 3376–3385
26 Laemmli, U. K. (1970) Nature (London) **227**, 680–685
27 Heakeshoven, J. and Dernick, R. (1988) Electrophoresis **9**, 28–32
28 Contreras, M. A., Bale, W. F. and Spar, I. L. (1983) Methods Enzymol. **92**, 277–292
29 Hilton, D. J. and Nicola, N. A. (1992) J. Biol. Chem. **267**, 10238–10247
30 Winzor, D. J. (1969) in Physical Principles and Techniques of Protein Chemistry, Part A, (Leach, S. J., ed.), pp. 451–495, Academic Press, New York
31 Modrell, B., Liu, J., Miller, H. and Shoyab, M. (1994) Growth Factors **11**, 81–91
32 Liu, J., Modrell, B., Aruffo, A., Scharnowske, S. and Shoyab, M. (1994) Cytokine **6**, 272–278
33 Clark, R. (1994) B.Sc. (Hons) Thesis, The University of Melbourne, Australia
34 Hoffman, R. C., Castner, B. J., Gerhart, M., Gibson, M. G., Rasmussen, B. D., March, C. J., Weatherbee, J., Tsang, M., Gustchina, A., Schalk-Hihi, C., Reshetnikova, L. and Wlodawer, A. (1995) Protein Sci. **4**, 382–386
35 Park, L. S., Friend, D., Sassenfeld, H. M. and Urdal, D. L. (1987) J. Exp. Med. **166**, 476–488
36 Kondo, M., Takeshita, T., Ishii, N., Nakamura, M., Watanabe, S., Arai, K. I. and Sugamura, K. (1993) Science **262**, 1874–1877
37 Russel, S. M., Keegan, A. D., Harada, N., Nakamura, Y., Noguchi, M., Leland, P., Friedmann, M. C., Miyajima, A., Puri, R. K., Paul, W. E. and Leonard, W. J. (1993) Science **262**, 1880–1883
38 Devos, R., Guisez, Y., Cornelis, S., Verhee, A., Van der Heyden, J., Manneberg, M., Lahm, H.-W., Fiers, W., Tavernier, J. and Plaetinck, X. (1993) J. Biol. Chem. **268**, 6581–6587
39 Johanson, K., Appelbaum, E., Doyle, M., Hensley, P., Zhao, B., Abdel-Meguid, S. S., Young, P., Cook, R., Carr, S., Matico, R., et al. (1995) J. Biol. Chem. **270**, 9459–9471
40 de Vos, A. M., Ultsch, M. and Kossiakoff, A. A. (1992) Science **255**, 306–312
41 Hudson, K. R., Vernallis, A. B. and Heath, J. K. (1996) J. Biol. Chem. **271**, 11971–11978
42 Tanigawa, T., Elwood, N., Metcalf, D., Cary, D., DeLuca, E., Nicola, N. A. and Begley, C. G. (1993) Proc. Natl. Acad. Sci. U.S.A. **90**, 7864–7868

Received 18 December 1996/6 March 1997; accepted 27 March 1997